Geophysical Research Letters

RESEARCH LETTER
10.1029/2024GL114313

Tree-Ring Stable Isotopes Reveal a Hydroclimate Shift in Eastern England Around 4.2 ka Ago

Tatiana Bebchuk[1], Otmar Urban[2], Tito Arosio[1], Alexander Kirdyanov[1,3], Ronny Friedrich[4], Natálie Pernicová[2], Josef Čáslavský[2], Mirek Trnka[2,5], Alis Francis[1], Mark Macklin[6], Jan Esper[2,7], and Ulf Büntgen[1,2,8]

[1]Department of Geography, University of Cambridge, Cambridge, UK, [2]Czech Academy of Sciences, Global Change Research Institute, Brno, Czech Republic, [3]Siberian Federal University, Krasnoyarsk, Russian Federation, [4]Curt-Engelhorn-Centre Archaeometry, Mannheim, Germany, [5]Department of Agrosystems and Bioclimatology, Faculty of AgriSciences, Mendel University in Brno, Brno, Czech Republic, [6]College of Health and Science, University of Lincoln, Lincoln, UK, [7]Department of Geography, Johannes Gutenberg University, Mainz, Germany, [8]Department of Geography, Faculty of Science, Masaryk University, Brno, Czech Republic

Abstract Tree ring-based climate reconstructions are fundamental for high-resolution paleoclimatology, but only a few of them extend back into the mid-Holocene (8,200–4,200 years BP). Here, we present annually-resolved tree-ring stable carbon and oxygen isotopes ($\delta^{13}C$ and $\delta^{18}O$) from subfossil yew (*Taxus baccata*) wood excavated in the Fenland region of eastern England. We develop an eco-physiological model to reconstruct hydroclimate variability from 5,224 to 4,813 ± 4 and 4,612–4,195 ± 6 cal. years BP. Our findings suggest that a relative sea-level rise in the North Sea, riverine flooding, and a prolonged negative phase of the North Atlantic Oscillation caused unusually wet conditions around 4,200 years ago when yew woodlands in eastern England disappeared. We expect our study to stimulate high-resolution stable isotope measurements in relict wood and encourage the integration of terrestrial and marine proxy archives to reconstruct the causes and consequences of large-scale climate variations around the still debated 4.2 ka event.

Plain Language Summary Understanding how the Earth's climate system has varied in the past is essential to predict future climate changes. In this study, we measured thousands of annually-resolved tree-ring widths and tree-ring stable isotopes in hundreds of subfossil yew trees excavated by generations of farmers in the Fenland region of eastern England. The exceptionally well-preserved wood archive, together with an innovative methodological approach allowed mid-Holocene hydroclimate variability to be reconstructed from circa 5,200–4,200 years ago. Our new paleoclimate record reveals unusually wet conditions around 4,200 years ago when yew woodlands in eastern England disappeared. Likely driven by a sea-level rise, riverine flooding, and a prolonged negative phase of the North Atlantic Oscillation, the observed environmental shift adds new insights into the period around the enigmatic 4.2 ka event. Our study also emphasizes the potential of stable isotopes in relict wood to reconstruct Holocene climate at high spatiotemporal resolution.

Key Points:

- Combining tree-ring widths (TRW) and tree-ring stable isotopes (TRSI) allows us to develop floating climate reconstructions
- A shift toward unusually wet conditions in eastern England coincided with the disappearance of yew woodlands around 4,200 years ago
- Hydroclimate variability over the North Atlantic provides new insights into the nature of the enigmatic 4.2 ka event

Supporting Information:

Supporting Information may be found in the online version of this article.

Correspondence to:

T. Bebchuk,
tb649@cam.ac.uk

Citation:

Bebchuk, T., Urban, O., Arosio, T., Kirdyanov, A., Friedrich, R., Pernicová, N., et al. (2025). Tree-ring stable isotopes reveal a hydroclimate shift in eastern England around 4.2 ka ago. *Geophysical Research Letters*, *52*, e2024GL114313. https://doi.org/10.1029/2024GL114313

Received 19 DEC 2024
Accepted 4 MAR 2025

Author Contributions:

Conceptualization: Tatiana Bebchuk, Otmar Urban, Tito Arosio, Ulf Büntgen
Formal analysis: Tatiana Bebchuk, Tito Arosio, Alexander Kirdyanov
Investigation: Tatiana Bebchuk, Ulf Büntgen
Methodology: Tatiana Bebchuk, Otmar Urban, Tito Arosio
Resources: Tatiana Bebchuk, Otmar Urban, Tito Arosio, Ronny Friedrich, Natálie Pernicová, Josef Čáslavský, Mirek Trnka, Alis Francis
Supervision: Ulf Büntgen
Visualization: Tatiana Bebchuk, Ulf Büntgen
Writing – original draft: Tatiana Bebchuk

© 2025. The Author(s).
This is an open access article under the terms of the Creative Commons Attribution License, which permits use, distribution and reproduction in any medium, provided the original work is properly cited.

1. Introduction

Although tree-ring chronologies are frequently used to develop annually-resolved and absolutely-dated climate reconstructions for the past millennium (Esper et al., 2016; Ljungqvist et al., 2020), only nine such records extend continuously back into the mid-Holocene. Six of these use tree-ring widths (TRW) to reconstruct summer precipitation in the western United States (Hughes & Graumlich, 1996) and summer temperatures on the Yamal peninsula (Hantemirov et al., 2021, 2022), Swedish Lapland (Grudd et al., 2002), Fennoscandia (Helama et al., 2012), the western United States (Salzer et al., 2014), and northern Patagonia (Lara et al., 2020). The other three studies utilize tree-ring stable isotopes (TRSI) to reconstruct cloud cover in Finland (Helama et al., 2018), monsoon rainfall on the Tibetan Plateau (Yang et al., 2021), and hydroclimate in the European Alps (Arosio et al., 2023). In addition, floating TRSI chronologies have shown a potential to be used for climate reconstructions, such as those for the Younger Dryas some 12 ka years ago (Panyushkina et al., 2008), the Early Pliocene some 4 million years ago (Ballantyne et al., 2006; Csank et al., 2011), and the Late Oligocene some 25 million years ago (Vornlocher et al., 2021). However, such reconstructions are only possible if climate signals captured by the different "growth-independent" TRSIs are interpreted using mechanistic understanding of eco-physiological processes (Büntgen, 2022; McCarroll & Loader, 2004).

Writing – review & editing: Tatiana Bebchuk, Otmar Urban, Tito Arosio, Alexander Kirdyanov, Mirek Trnka, Mark Macklin, Jan Esper, Ulf Büntgen

The Fenland in eastern England is a worldwide unique region for archeological, paleoecological, and dendrochronological research. Situated between Cambridge in the south and Lincoln in the north, the flat lowland covered with deep peaty soils provides a rich paleoenvironmental archive. Extensive archeological surveys began as early as in the 1870s (Miller & Skertchly, 1878) and resulted in a collection of thousands of objects spanning human history from the Paleolithic to the Medieval period (Brown, 2000; Glazebrook, 1997; Medlycott, 2011). A dense network of soil cores has revealed a complex evolution of vegetation cover on a mosaic-like landscape (Godwin, 1940; Waller, 1994) and facilitated detailed reconstruction of sea-level changes of the North Sea during the Holocene (Shennan, 1986; Shennan et al., 2018). Excavated from agricultural fields, relict oak trunks, so-called "bog oaks", were used to develop a 1500-year long TRW chronology for the mid-Holocene (Baillie & Brown, 1988), and a recent finding of hundreds of well-preserved yew trunks has further advanced regional dendrochronological records (Bebchuk et al., 2024). Despite the long tradition of archeological and paleoenvironmental research and the abundant subfossil wood, TRSI have never been measured in the Fenland.

Here, we present carbon ($\delta^{13}C$) and oxygen ($\delta^{18}O$) TRSI in subfossil yew (*Taxus baccata* L.) wood from the Fenland. We develop an eco-physiological model to understand how climate and environmental conditions affect TRSI and TRW, and use it to reconstruct hydroclimate variability during the mid-Holocene in eastern England. We then compare our reconstruction with independent proxy evidence of sea-level change, riverine flooding, and atmospheric circulation patterns.

2. Data and Methods

Over 400 well-preserved subfossil yew trunks were excavated from peat-rich soils in the coastal lowland region of eastern England (Figures 1a and 1b) (Bebchuk et al., 2024). Dendrochronological cross-dating, supplemented with 60 annually-resolved radiocarbon (^{14}C) dates, resulted in two floating TRW chronologies that integrate 36 and 48 relict yew trees and span 5,224−4,813 ± 4 and 4,612−4,195 ± 6 calibrated (cal.) years BP (hereafter "early" and "late" chronologies), respectively. The TRW chronologies, as well as further steps performed in the study are depicted on a flowchart in Figure 1c.

Fifteen yew trees from the end of the late chronology with wide and regular growth rings were selected for $\delta^{13}C$ and $\delta^{18}O$ measurements (Figure S1 in Supporting Information S1). Annual rings were split under a stereo microscope, and each ring, containing early- and late-wood was weighed at 0.001 mg precision. A minimum of 3.0 mg per sample were required to extract 0.7 mg of alpha-cellulose for individual $\delta^{13}C$ and $\delta^{18}O$ measurements according to a modified Jayme-Wise isolation method (Boettger et al., 2007). Each sample underwent two separate washes in a 5% NaOH solution for 2 hr at 60°C, followed by an additional 30-hr treatment in a 7% $NaClO_2$ solution. To maintain the pH between 4 and 5, acetic acid (99.8%) was added throughout the process. The samples were then dried at 50°C for 24 hr and stored in Eppendorf microtubes. For $\delta^{13}C$ analysis, the 0.7 mg alpha-cellulose was placed into tin capsules and combusted to CO_2 at 960°C. For $\delta^{18}O$ analysis, the same amount of cellulose was placed in silver capsules and pyrolyzed to CO at 1,450°C. Stable isotopes in the CO_2 and CO gases were measured with an ISOPRIME100 continuous flow isotope ratio mass spectrometer (IRMS; IsoPrime, Manchester, UK). Prior to each set of analyses, the IRMS was tuned and tested for stability (standard deviation ≤0.04‰ over 10 pulses of reference gas) and linearity (≤0.03‰/nA) over the expected ion current range obtained from the measurements of the test samples. Measurement precision was maintained with standard deviations ≤0.06‰ for $\delta^{13}C$ and ≤0.10‰ for $\delta^{18}O$, based on five consecutive measurements of the same alpha-cellulose sample. Isotopic values were calibrated against certified reference materials from the International Atomic Energy Agency (IAEA, Vienna, Austria) and the United States Geological Survey (USGS, USA). The $\delta^{13}C$ values were standardized against caffeine (IAEA-600) and graphite (USGS24), while $\delta^{18}O$ values were referenced to benzoic acids (IAEA-601 and IAEA-602). Carbon and oxygen ratios are reported in permil (‰) relative to the Vienna Pee Dee Belemnite (VPDB) and Vienna Standard Mean Ocean Water (VSMOW), respectively (Coplen, 1995).

Raw TRW and TRSI series exhibit age-related trends (Figure S2 in Supporting Information S1). To remove the age-related trends from TRW series, we used age-dependent splines with an initial stiffness of 50 years (Melvin, 2004). For TRSI series, we applied the Regional Curve Standardization method (Briffa et al., 1992) that retains possible low-frequency variability in the data and preserves the level-offset between samples (following Büntgen, 2022; and as in Esper et al., 2003; Helama et al., 2018; Arosio et al., 2023). We further stabilized the

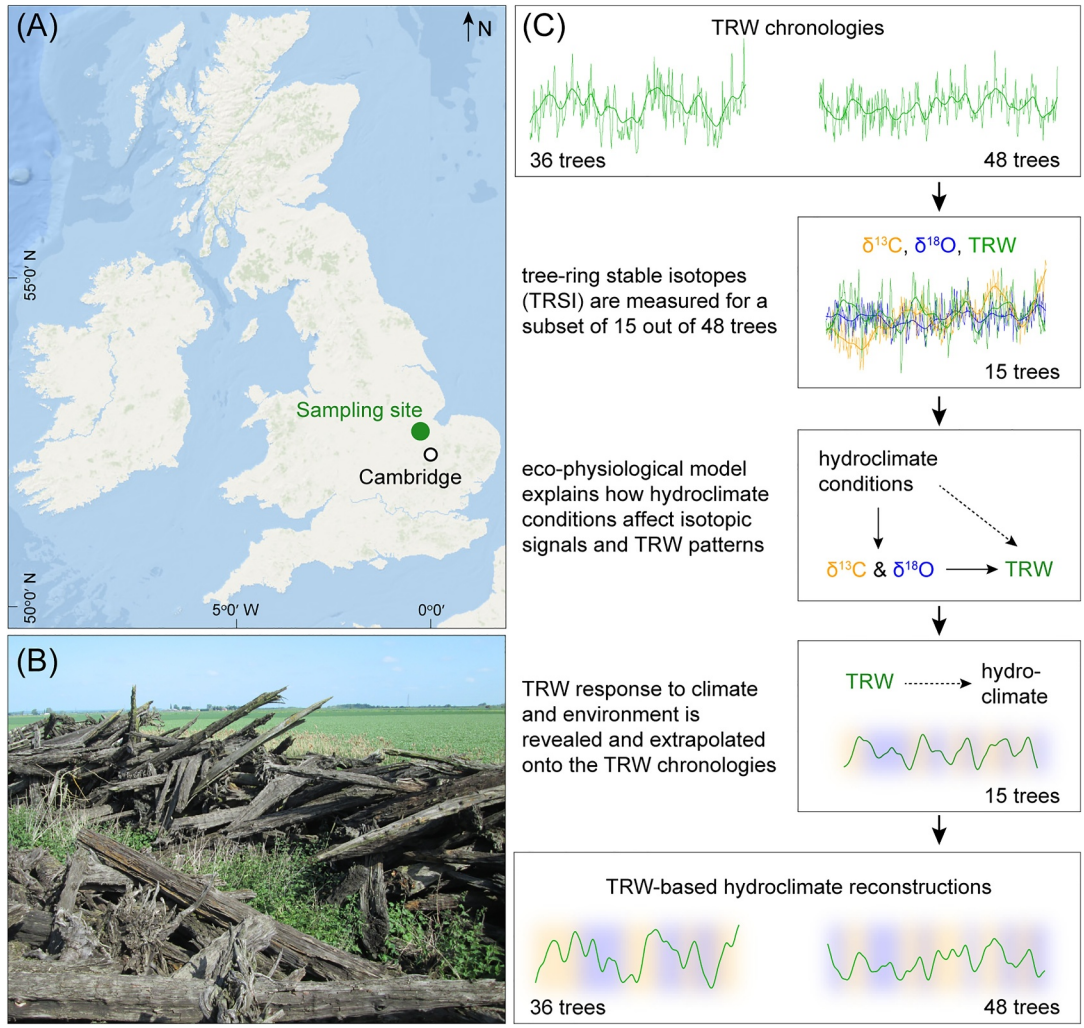


Figure 1. Map of the British Isles with the sampling site location (a) and photo of a pile of yew trunks (b). Panel (c) shows a flowchart explaining the steps performed in the study from top to bottom: two floating tree-ring width (TRW) chronologies are developed, tree-ring stable isotopes (TRSI) are measured for a subset of 15 trees from the late (right side) chronology, an eco-physiological model is established to explain how TRSI signals change depending on climate and environmental conditions and how TRW patterns correspond to these conditions. Finally, TRW response to hydroclimate is used to develop reconstructions for both, the early and the late TRW chronologies.

variance by dividing the mean of the resulting TRW, $\delta^{13}C$, and $\delta^{18}O$ chronologies by their respective 30-year moving standard deviations (Büntgen et al., 2024).

We developed an eco-physiological model to interpret the TRSI and TRW chronologies in response to environmental conditions. Our model builds upon established mechanistic models that explain the impact of climatic and environmental drivers on TRSI signals (Gessler et al., 2014; Roden et al., 2000; Scheidegger et al., 2000; Siegwolf et al., 2023). We distinguished four types of TRSI changes: (a) both $\delta^{13}C$ and $\delta^{18}O$ increase, (b) $\delta^{13}C$ increases while $\delta^{18}O$ decreases, (c) $\delta^{13}C$ decreases while $\delta^{18}O$ increases, and (d) both $\delta^{13}C$ and $\delta^{18}O$ decrease. Each pattern was linked to Fenland-specific scenarios of climate and environmental changes, along with the corresponding stomatal responses and gas exchanges between the atmosphere and leaf interior that contribute to the observed TRSI signals (Figure 2).

Scenario 1 refers to atmospheric dryness during which vapor pressure deficit (VPD) rises, leading to a decrease in stomatal conductance (i.e., closure of the stomatal aperture), especially strong under limited soil water availability. Stomatal closure limits CO_2 diffusion into the leaf interior, causing the photosynthetic demand for CO_2 to exceed its supply and resulting in a decrease in inter-cellular CO_2 concentration. This decrease in CO_2 availability

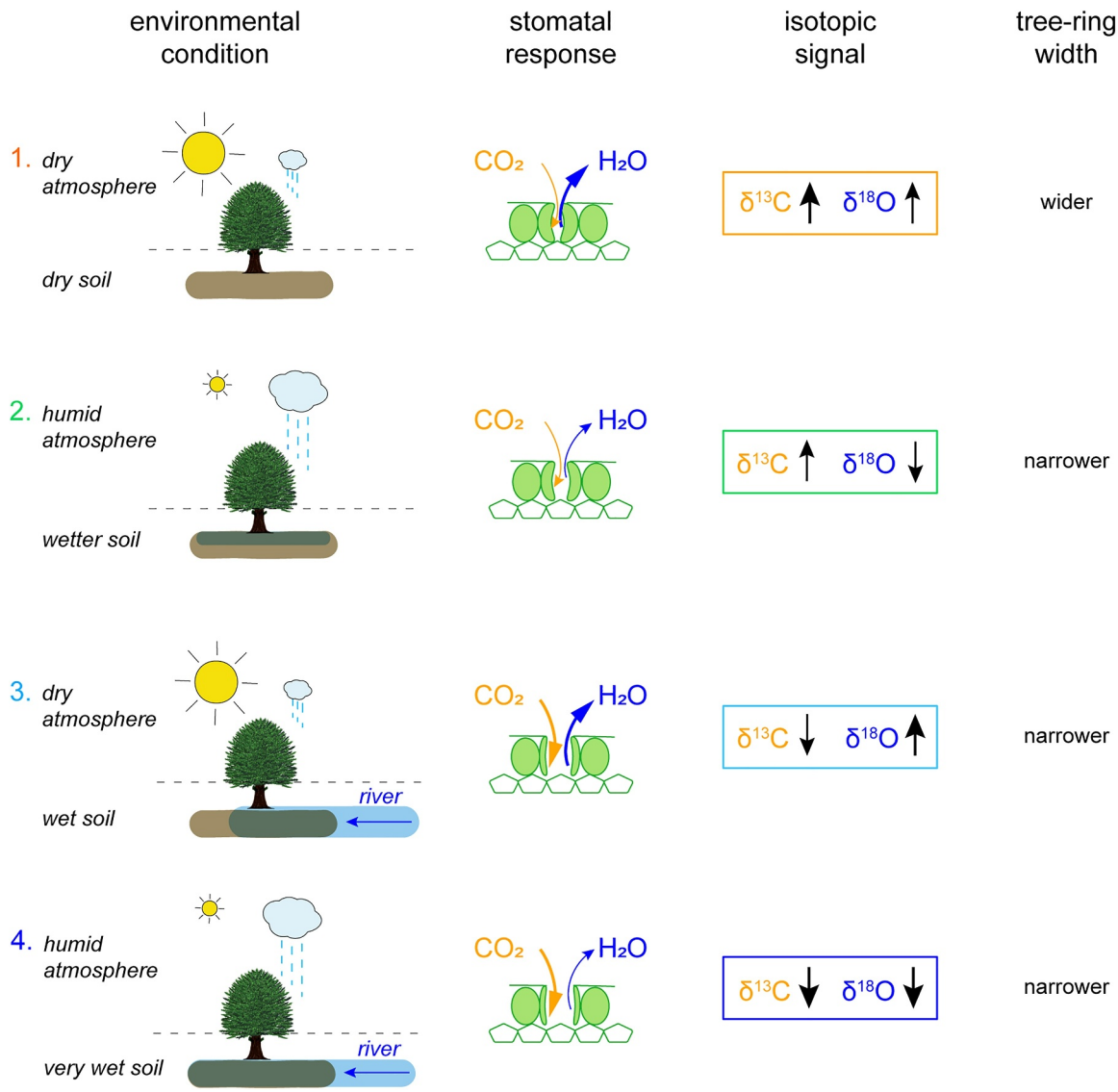


Figure 2. From left to right, the table shows environmental factors, stomatal responses, isotopic signals, and tree-ring width patterns. The leftmost column presents four predefined scenarios of the Fenland environmental conditions, with varying atmospheric humidity and soil wetness (for details, see text). The second column illustrates the degree of stomatal opening or closure in response to environmental conditions, with arrow thickness representing the relative rate of CO_2 and H_2O gas exchange. The third column presents the stable isotopes' behavior, and the rightmost column shows the tree-ring width signal revealed from the combination of the two stable isotopes chronologies.

reduces ^{13}C discrimination during photosynthesis, thereby increasing $\delta^{13}C$ values of the synthesized cellulose (Farquhar et al., 1980). Despite the partially closed stomata, transpiration rates can remain high in dry atmospheres, as water flow is driven by the steep water potential gradient across the soil-plant-atmosphere continuum. Under high transpiration rates, water molecules containing the lighter ^{16}O isotope evaporate preferentially over those containing the heavier ^{18}O isotope, leading to an increase in $\delta^{18}O$ values in synthesized cellulose (Scheidegger et al., 2000). As a result, both $\delta^{13}C$ and $\delta^{18}O$ ratios increase (Figure 2).

Scenario 2 refers to conditions of increased precipitation, high air humidity, lower temperatures, and a decrease in atmospheric VPD. Although VPD values are low, the stomata remain relatively closed due to reduced light intensities caused by cloudy skies, which limit CO_2 diffusion into leaves (Mott et al., 2008) and decrease the intercellular CO_2 concentration. The overall wetter conditions lead to reduced transpiration rates and generally lower $\delta^{18}O$ ratios (Martínez-Sancho et al., 2023; Roden et al., 2000). As a result, $\delta^{13}C$ ratios moderately increase, while $\delta^{18}O$ ratios decrease (Figure 2).

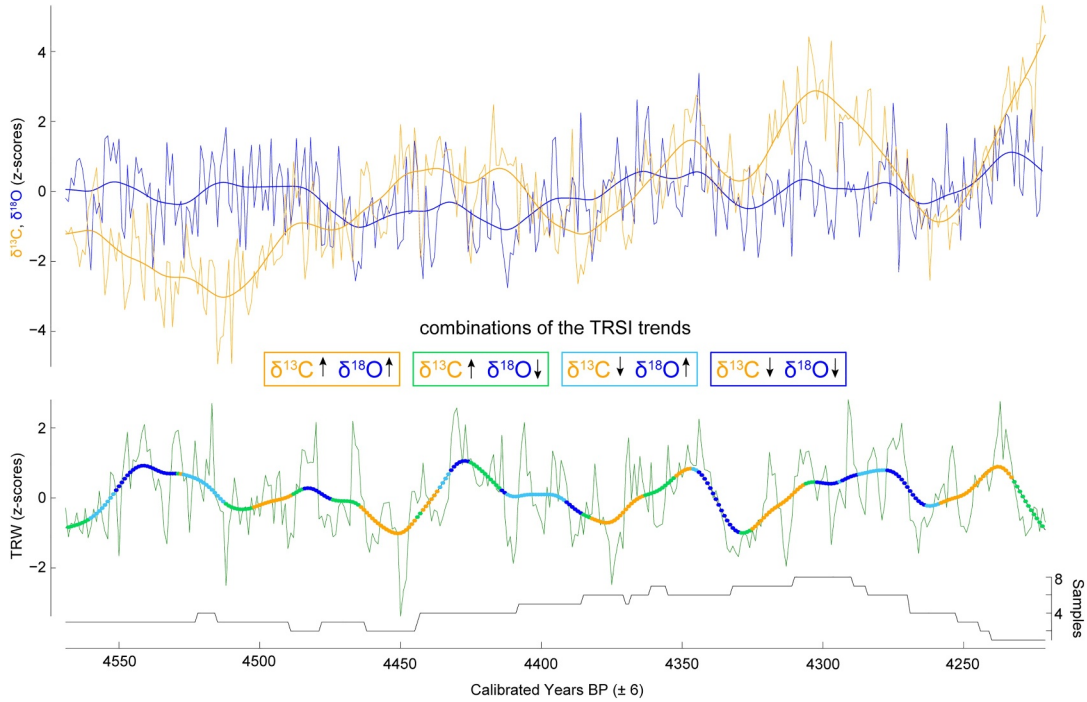


Figure 3. The upper panel presents normalized $\delta^{13}C$ (orange) and $\delta^{18}O$ (blue) chronologies with 30-year splines highlighting the long-term variability. The bottom panel shows the TRW chronology (green) and a 30-year spline colored depending on the combination of the TRSI changes: both isotopes increase (orange), $\delta^{13}C$ increases and $\delta^{18}O$ decreases (green), $\delta^{13}C$ increases and $\delta^{18}O$ decreases (light blue), and both isotopes decrease (blue). Note the colors correspond to those in Figure 2. The sample replication of the three chronologies is shown in black.

Scenario 3 refers to dry atmospheric conditions combined with elevated groundwater tables caused by sea-level rise in the North Sea, leading to wet soils (Bebchuk et al., 2024). Despite an increased VPD, stomata remain relatively open due to a high availability of soil moisture, ensuring sufficient water and CO_2 supplies to the leaf tissues (Ding et al., 2021). Accordingly, photosynthesis operates at relatively high concentrations of inter-cellular CO_2, leading to increased ^{13}C discrimination and a corresponding decrease in $\delta^{13}C$ values. At the same time, very high transpiration rates result in rising $\delta^{18}O$. As a result, $\delta^{13}C$ ratios decrease, while $\delta^{18}O$ ratios increase (Figure 2).

Scenario 4 refers to sea-level and groundwater table rises that coincide with colder and wetter atmospheric conditions. The stomata remain open, and the CO_2 supply substantially exceeds the demand for photosynthesis, leading to high concentrations of inter-cellular CO_2, enhanced ^{13}C discrimination, and a decrease in $\delta^{13}C$ values. Transpiration rates are reduced and thus, $\delta^{18}O$ ratios decrease. As a result, both $\delta^{13}C$ and $\delta^{18}O$ ratios decrease (Figure 2).

For developing a climate reconstruction, we used a combination of the carbon and oxygen TRSI chronologies smoothed with a 30-year spline (Figure 3a). We produced a timeseries illustrating how the four scenarios changed over time (Figure 3b). We then compared it with a TRW chronology developed from the same 15 trees to establish growth-climate relationships (Figure 3b). The observed TRW-climate relationships were further extended onto both the early and the late TRW chronologies (a reader is referred to the Figure 1c for the sketch of the methodology). Finally, we compared our new hydroclimate reconstructions against independent records of relative sea-level (RSL) changes in the North Sea (Shennan et al., 2018) and the North Atlantic Oscillation (NAO) (Becker et al., 2020). The RSL reconstruction was derived from marine index points over the Fenland region (Waller, 1994), for which radiocarbon dates were recalibrated with the OxCal v4.4.4 software (Bronk Ramsey, 2021) against the most recent IntCal20 calibration curve (Reimer et al., 2020). The NAO variability was reconstructed from sediment cores from the south-eastern Norwegian Sea.

3. Results and Discussion

The $\delta^{13}C$ and $\delta^{18}O$ chronologies span 378 years from 4,584–4,206 ± 6 cal. years BP with a sample replication ranging from 1 to 8 series (Figure 2a, Figure S3 in Supporting Information S1). The mean $\delta^{13}C$ values tend to be 1–4‰ higher than those reported from other mid-Holocene wood samples, such as Irish oaks (McCormac et al., 1994) and Fennoscandian pines (Edvardsson et al., 2014; Torbenson et al., 2022). In contrast, the mean $\delta^{18}O$ values are 1–4‰ lower than those observed in mid-Holocene pines from Sweden (Edvardsson et al., 2014), larch and pines from the Alps (Arosio, Ziehmer-Wenz, et al., 2020), and juniper trees from the Tibetan Plateau (Yang et al., 2021). We suppose that the differences in $\delta^{13}C$ arise from species-specific photosynthetic properties (Arosio et al., 2024; McCarroll & Loader, 2004), whereas the differences in $\delta^{18}O$ likely reflect variations in climate conditions and the isotopic composition of precipitation (Arosio et al., 2024; Saurer et al., 2002).

The age-related trends in yew TRSI series contribute to the ongoing debate about whether TRSI data should be detrended before being used for climate reconstructions (initiated in Esper et al., 2010). Although some TRSI data sets, such as living and relict oaks from the Czech Republic (Büntgen et al., 2020), exhibit no age-dependant behavior, other studies report pronounced TRSI changes with cambial age (Helama et al., 2018; Wieland et al., 2024). We found significant correlations between the cambial age and the mean of the age-aligned raw series (Pearson's correlation coefficient of 0.86 for $\delta^{13}C$ and 0.13 for $\delta^{18}O$; $p < 0.001$), normalized series (0.93, 0.39), and normalized series trimmed by the sample replication ≥5 (0.91, 0.54). Moreover, 10,000 Monte Carlo simulations confirmed the presence of these trends, with linear interpolation slopes of 0.01 for $\delta^{13}C$ and 0.003 for $\delta^{18}O$ per year. Our findings align with a general view that age-related trends are more pronounced in $\delta^{13}C$ than in $\delta^{18}O$. For example, Helama et al. (2015) and Kern et al. (2023) found strong age-related trends in $\delta^{13}C$ but not $\delta^{18}O$ in subfossil pines from Finland and Romania, respectively. Similarly, moderate age-related trends in $\delta^{18}O$ were observed in relict pines from Fennoscandia (Torbenson et al., 2022), while Arosio, Ziehmer, et al. (2020) concluded that these trends can be species-specific for Alpine pine and larch. Our results emphasize the importance of investigating age-related trends in TRSI series across plant species and regions before developing TRSI-based climate reconstructions (Esper et al., 2010).

Our eco-physiological model shows that changes in $\delta^{13}C$ and $\delta^{18}O$ are primarily driven by soil and atmospheric moisture, respectively. The $\delta^{13}C$ chronology exhibits an upward trend from −22.4‰ to −20.1‰, with marked decreases around 4,520, 4,380 and 4,260 cal. years BP (Figure 3a). These depressions likely indicate groundwater influx caused by an RSL rise in the North Sea, which impeded free passage of Fenland rivers into the Wash bay and elevated regional groundwater tables (Bebchuk et al., 2024). Then, as peat accumulated and soils were drying, $\delta^{13}C$ values gradually rose. The $\delta^{18}O$ chronology represents a joint moisture signal of precipitation and river water since their isotopic values were found to be similar in eastern England (Darling et al., 2003), and the local drainage basin ensures minimal seasonal $\delta^{18}O$ variations (Orr et al., 2007). The relative invariability of $\delta^{18}O$ chronology suggests no major changes in atmospheric circulation and a consistent soil water source throughout time. This finding implies that possible saltwater intrusion, which would otherwise have altered the isotopic signature of the source water (Ellsworth & Sternberg, 2014; Lovelock et al., 2017), did not have a direct effect on yew woodlands.

Relatively dry atmospheric and soil conditions (Scenario 1) favored yew growth, whereas reduced TRW coincided with periods of increased groundwater tables and wetter soil conditions (Scenarios 2–4) (Figure 2). Our findings align with previous studies that link reduced TRW in pines and oaks from peatbogs in Ireland, Germany, Denmark, and Sweden to rising groundwater tables during the mid-Holocene (Eckstein et al., 2009; Edvardsson et al., 2016; Leuschner et al., 2002; Pilcher et al., 1995). Moreover, several studies show that excessive soil moisture (Scenarios 3 and 4) reduces the likelihood of yew seedlings to establish and survive (Bujoczek & Bujoczek, 2018), and the combination of low temperatures and diffuse light (Scenarios 2 and 4) is probably a direct reason for higher yew mortality (Iszkuło, 2010). These growth-climate relationships, however, are contrary to those observed in modern yew trees in southeast England (Bebchuk et al., 2025), because an extensive drainage in the 17–19th centuries altered the hydroclimate regime of the region (Fowler, 1933; Waller, 1994). Consequently, calibration trials with living trees could be misleading.

Our final TRW-based hydroclimate reconstruction spans 828 years from 5,224–4,813 ± 4 and 4,612–4,195 ± 6 cal. years BP (Figure 4a). Despite a range of methodological limitations, including low TRSI sample replication and discontinuous TRW record, the reconstruction represents the best possible high-resolution approximation of mid-Holocene droughts and pluvials in eastern England and north-western Europe. The

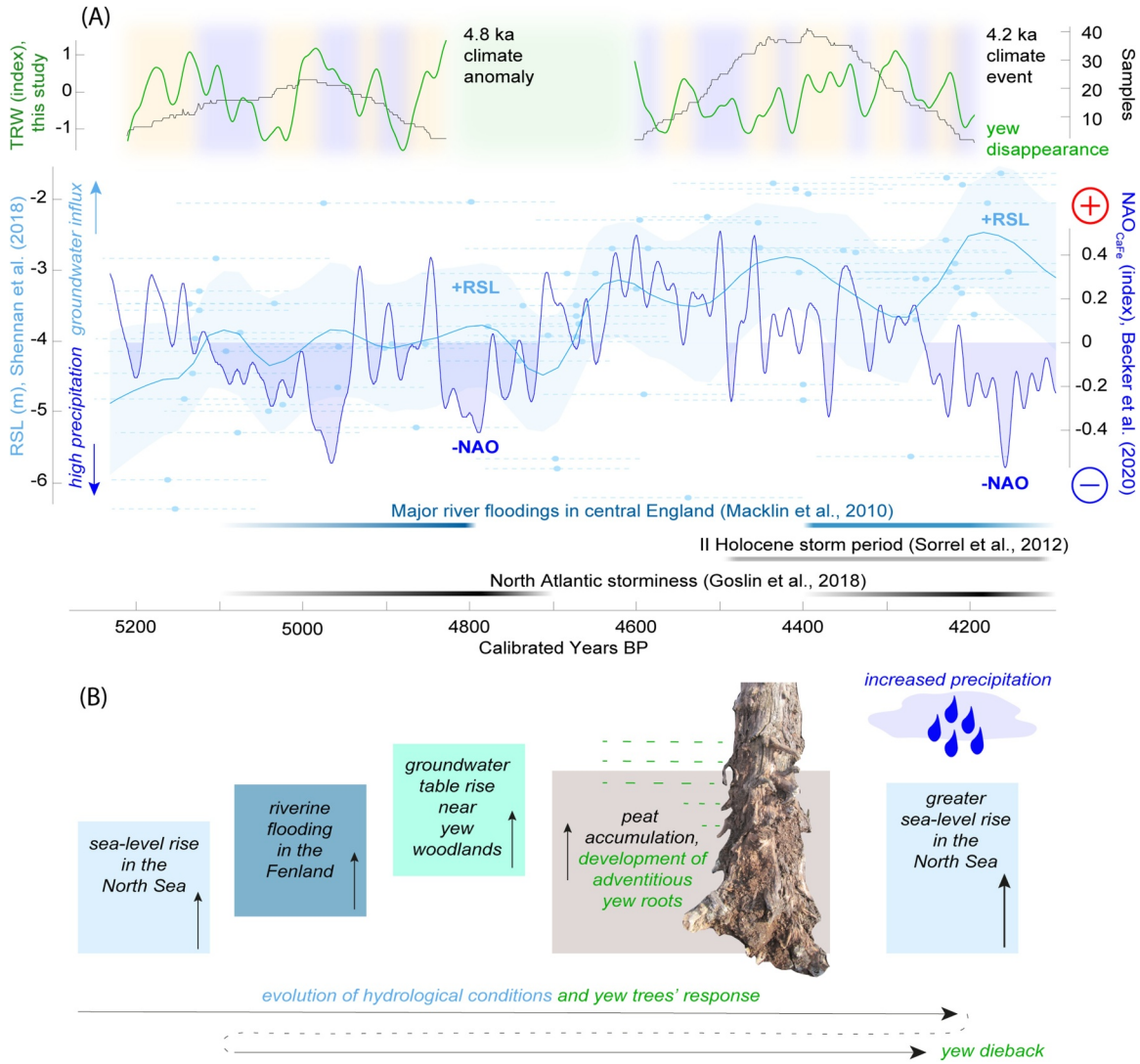


Figure 4. (a) Our TRW-based hydroclimate reconstruction (green; sample replication in black) with reconstructed phases of Fenland dry (Scenario 1; yellow bars) and humid (Scenarios 2, 3, and 4; purple bars) conditions. Note the early part is based on the extrapolation of growth-climate relationships identified in the late part. The reconstruction of relative sea-level (RSL, m) changes in the North Sea (light blue) is based on the data from the Fenland specifically, after Shennan et al. (2018). Marine index points of RSL (dots) are shown with a temporal uncertainty (dashed line), a smoothing mean (solid line) and its vertical uncertainty (zone). The reconstruction of the winter North Atlantic Oscillation (NAO) variability (blue) is based on a sediment core from western Norway, after Becker et al. (2020). The NAO_{CaFe} index bandpass filtered with a cut-off of 10–500 is shown as an inverted plot with negative NAO phases in blue. Note yew disappearance around 4,200 cal. years BP and corresponding RSL and NAO conditions labeled. Major riverine flooding after Macklin et al. (2010) and storminess in the North Atlantic after Sorrel et al. (2012) and Goslin et al. (2018) are shown as blue and gray horizontal bars, respectively. The climate anomaly around 4.8 ka BP and the 4.2 ka climate event are marked. (b) Evolution of paleo-environmental conditions in the Fenland and their impact on yew growth.

record reveals a hydroclimate shift toward unusually wet conditions that eventually caused yew disappearance around 4,200 cal. years BP (Figure 4a). This period coincided with an RSL rise in the North Sea (Shennan et al., 2018) and a prolonged negative phase of the NAO (Becker et al., 2020). The Holocene fluvial record for central England exhibits major riverine flooding between 4,400 and 4,100 cal. years BP (Macklin et al., 2010), thereby providing independent evidence for an RSL rise. Mid-Holocene RSL fluctuations, which occurred without significant meltwater influxes, are usually associated with increased storminess (Uścinowicz et al., 2022). Sorrel et al. (2012) identified the period 4,500−3,950 cal. years BP as the "Second Holocene Storm Period", using data from North Sea coastal sediments, and Goslin et al. (2018) reported increased storminess in the North Atlantic at 4,400−4,100 centered around 4,200 cal. years BP (Figure 4a). Although negative phases of the NAO are commonly associated with reduced precipitation over the British Isles (Wanner et al., 2001), central and

eastern England may receive more precipitation during negative NAO conditions (West et al., 2019, 2022). We therefore conclude that yew trees coped with short-term waterlogged conditions by producing adventitious roots visible on at least 10% of the excavated trunks (Figure 4b; Bebchuk et al., 2024; Jackson, 1955). However, a joint occurrence of a prolonged negative NAO phase and a sea-level rise in the North Sea would have led to long-lasting inundation, resulting in hypoxia or anoxia and possibly spread of *Phytophthora* (Hansen et al., 2012), a disease known to damage yew roots (Torgeson et al., 1954), and triggering dieback (Figure 4b; Bujoczek & Bujoczek, 2018).

The shift toward wetter conditions around 4,200 cal. years BP coincided with the so-called "4.2 ka event" (Staubwasser et al., 2003; Weiss et al., 1993), which has been coined as a climatological divide between the Middle and Late Holocene (Walker et al., 2019). This event is characterized by extremely dry conditions in Asia and Africa that are believed to have contributed to a collapse of several ancient civilizations in Northern Hemisphere mid-latitudes (Chen et al., 2023; Weiss et al., 1993). In contrast, evidence from varved lake sediments in Poland indicates a pronounced cooling (Zander et al., 2024), and both wetter and drier anomalies have been identified in the Mediterranean region (Bini et al., 2019). However, no compelling evidence for unusual climate change has been previously reported for the British Isles (Roland et al., 2014) and the northern North Atlantic (Bradley & Bakke, 2019). A similar combination of increased storminess (Goslin et al., 2018), riverine flooding (Macklin et al., 2010), and prolonged negative NAO conditions (Becker et al., 2020) seems to have also occurred around 4,800 cal. years BP (Figure 4a). Although this period coincides with a suite of warm and wet climate anomalies reported by McKay et al. (2024), no definitive conclusion can be drawn from our new paleoclimate record whose early part ceases around 4,800 cal. years BP. Bridging the two floating yew chronologies is needed to further understand mid-Holocene climate and environmental conditions in eastern England.

Data Availability Statement

Early and late tree-ring width chronologies are available at the International Tree-Ring DataBase (ITRDB) at https://www.ncei.noaa.gov/access/paleo-search/study/41019 and https://www.ncei.noaa.gov/access/paleo-search/study/41020, respectively. Raw tree-ring stable isotopes are published at the NOAA for Paleoclimatology data repository at https://www.ncei.noaa.gov/access/paleo-search/study/41021. The reconstruction of relative sea-level changes can be found in the Supplementary material of the paper by Shennan et al. (2018). The reconstruction of NAO variability by Becker et al. (2020) is available from the PANGAEA data repository.

Acknowledgments
TB was funded by the Hill Foundation Cambridge Trust, TA by SNSF P500PN_210716, JE and UB received funding from the Czech Science Foundation (#23-08049S; Hydro8), the ERC Advanced Grant (# 882727; Monostar), and the ERC Synergy Grant (# 101118880; Synergy-Plague). The stable isotope measurements were supported by the Ministry of Education, Youth, and Sports of the Czech Republic through the CzeCOS program, Grant Nnumber LM2023048. The authors thank Inna Roshka for her work in the isotope laboratory. The authors declare that they have no known competing financial interests or personal relationships that could have appeared to influence the work reported in this paper.

References

Arosio, T., Büntgen, U., Nicolussi, K., Moseley, G. E., Saurer, M., Pichler, T., et al. (2024). Tree-ring $\delta^{18}O$ and $\delta^{2}H$ stable isotopes reflect the global meteoric water line. *Frontiers of Earth Science*, *12*. https://doi.org/10.3389/feart.2024.1440064

Arosio, T., Nicolussi, K., Leuenberger, M., Krusic, P. J., Esper, J., & Büntgen, U. (2023). Holocene-long climate signals in tree-ring stable isotopes from the European Alps. EGU-8180. https://doi.org/10.5194/egusphere-egu23-8180

Arosio, T., Ziehmer, M. M., Nicolussi, K., Schlüchter, C., & Leuenberger, M. (2020). Alpine Holocene tree-ring dataset: Age-related trends in the stable isotopes of cellulose show species-specific patterns. *Biogeosciences*, *17*(19), 4871–4882. https://doi.org/10.5194/bg-17-4871-2020

Arosio, T., Ziehmer-Wenz, M. M., Nicolussi, K., Schlüchter, C., & Leuenberger, M. (2020). Larch cellulose shows significantly depleted hydrogen isotope values with respect to evergreen conifers in contrast to oxygen and carbon isotopes. *Frontiers of Earth Science*, *8*, 523073. https://doi.org/10.3389/feart.2020.523073

Baillie, M. G. L., & Brown, D. M. (1988). An overview of oak chronologies. In *Science and Arhaeology. Presented at the Science and Arhaeology*. B.A.R. British Series 196. Glasgow, 1987.

Ballantyne, A. P., Rybczynski, N., Baker, P. A., Harington, C. R., & White, D. (2006). Pliocene Arctic temperature constraints from the growth rings and isotopic composition of fossil larch. *Palaeogeography, Palaeoclimatology, Palaeoecology*, *242*(3–4), 188–200. https://doi.org/10.1016/j.palaeo.2006.05.016

Bebchuk, T., Krusic, P. J., Pike, J. H., Piermattei, A., Friedrich, R., Wacker, L., et al. (2024). Sudden disappearance of yew (*Taxus baccata*) woodlands from eastern England coincides with a possible climate event around 4.2 ka ago. *Quaternary Science Reviews*, *323*, 108414. https://doi.org/10.1016/j.quascirev.2023.108414

Bebchuk, T., Moir, A. K., Arosio, T., Kirdyanov, A. V., Torbenson, M. C. A., Krusic, P. J., et al. (2025). *Taxus* tree-ring chronologies from southern England reveal western European hydroclimate changes over the past three centuries. *Climate Dynamics*, *63*(2), 108. https://doi.org/10.1007/s00382-025-07601-2

Becker, L. W. M., Sejrup, H. P., Hjelstuen, B. O., Haflidason, H., Kjennbakken, H., & Werner, J. P. (2020). Palaeo-productivity record from Norwegian Sea enables North Atlantic Oscillation (NAO) reconstruction for the last 8000 years. *npj Climate and Atmospheric Science*, *3*, 1–12. https://doi.org/10.1038/s41612-020-00147-6

Bini, M., Zanchetta, G., Perşoiu, A., Cartier, R., Català, A., Cacho, I., et al. (2019). The 4.2 ka BP event in the mediterranean region: An overview. *Climate of the Past*, *15*(2), 555–577. https://doi.org/10.5194/cp-15-555-2019

Boettger, T., Haupt, M., Knöller, K., Weise, S. M., Waterhouse, J. S., Rinne, K. T., et al. (2007). Wood cellulose preparation methods and mass spectrometric analyses of $\delta^{13}C$, $\delta^{18}O$, and nonexchangeable $\delta^{2}H$ values in cellulose, sugar, and starch: An interlaboratory comparison. *Analytical Chemistry*, *79*(12), 4603–4612. https://doi.org/10.1021/ac0700023

Bradley, R. S., & Bakke, J. (2019). Is there evidence for a "4.2 ka BP event" in the northern North Atlantic region? *Climate of the Past*, *15*(5), 1665–1676. https://doi.org/10.5194/cp-15-1665-2019

Briffa, K. R., Jones, P. D., Bartholin, T. S., Eckstein, D., Schweingruber, F. H., Karlén, W., et al. (1992). Fennoscandian summers from AD 500: Temperature changes on short and long timescales. *Climate Dynamics*, *7*(3), 111–119. https://doi.org/10.1007/BF00211153

Bronk Ramsey, C. (2021). OxCal v4. 4.4. Retrieved from https://c14.arch.ox.ac.uk/oxcal.html

Brown, N. (2000). Research and archaeology: A framework for the eastern counties 2. In J. Glazebrook (Ed.), *Research agenda and strategy*. East Anglian Archaeology.

Bujoczek, L., & Bujoczek, M. (2018). The dynamics of the *Taxus baccata* L. population and the factors affecting its regeneration in the Jasień Nature Reserve. *Dendrobiology*, *80*, 24–36. https://doi.org/10.12657/denbio.080.003

Büntgen, U. (2022). Scrutinizing tree-ring parameters for Holocene climate reconstructions. *WIREs Climate Change*, *13*(4), e778. https://doi.org/10.1002/wcc.778

Büntgen, U., Kolář, T., Rybníček, M., Koňasová, E., Trnka, M., Ač, A., et al. (2020). No age trends in oak stable isotopes. *Paleoceanography and Paleoclimatology*, *35*(4), e2019PA003831. https://doi.org/10.1029/2019PA003831

Büntgen, U., Reinig, F., Verstege, A., Piermattei, A., Kunz, M., Krusic, P., et al. (2024). Recent summer warming over the western Mediterranean region is unprecedented since medieval times. *Global and Planetary Change*, *232*, 104336. https://doi.org/10.1016/j.gloplacha.2023.104336

Chen, X., Deng, W., Xiao, H., Guo, H., Zeng, T., Zhao, J., & Wei, G. (2023). Coral paleoclimate perspectives support the role of low-latitude forcing on the 4.2 ka BP event. *Geophysical Research Letters*, *50*(13), e2023GL104010. https://doi.org/10.1029/2023GL104010

Coplen, T. B. (1995). New IUPAC guidelines for the reporting of stable hydrogen, carbon, and oxygen isotope-ratio data. *Journal of Research of the National Institute of Standards and Technology*, *100*(3), 285. https://doi.org/10.6028/jres.100.021

Csank, A. Z., Patterson, W. P., Eglington, B. M., Rybczynski, N., & Basinger, J. F. (2011). Climate variability in the Early Pliocene Arctic: Annually resolved evidence from stable isotope values of sub-fossil wood, Ellesmere Island, Canada. *Palaeogeography, Palaeoclimatology, Palaeoecology*, *308*(3–4), 339–349. https://doi.org/10.1016/j.palaeo.2011.05.038

Darling, W. G., Bath, A. H., & Talbot, J. C. (2003). The O and H stable isotope composition of freshwaters in the British Isles. 2. Surface waters and groundwater. *Hydrology and Earth System Sciences*, *7*, 183–195. https://doi.org/10.5194/hess-7-183-2003

Ding, Y., Nie, Y., Chen, H., Wang, K., & Querejeta, J. I. (2021). Water uptake depth is coordinated with leaf water potential, water-use efficiency and drought vulnerability in karst vegetation. *New Phytologist*, *229*(3), 1339–1353. https://doi.org/10.1111/nph.16971

Eckstein, J., Leuschner, H. H., Bauerochse, A., & Sass-Klaassen, U. (2009). Subfossil bog-pine horizons document climate and ecosystem changes during the Mid-Holocene. *Dendrochronologia, EuroDendro 2008: The long history of wood utilization*, *27*(2), 129–146. https://doi.org/10.1016/j.dendro.2009.06.007

Edvardsson, J., Edwards, T. W. D., Linderson, H., & Hammarlund, D. (2014). Exploring climate forcing of growth depression in subfossil South Swedish bog pines using stable isotopes. *Dendrochronologia*, *32*(1), 55–61. https://doi.org/10.1016/j.dendro.2013.08.002

Edvardsson, J., Stoffel, M., Corona, C., Bragazza, L., Leuschner, H. H., Charman, D. J., & Helama, S. (2016). Subfossil peatland trees as proxies for Holocene palaeohydrology and palaeoclimate. *Earth-Science Reviews*, *163*, 118–140. https://doi.org/10.1016/j.earscirev.2016.10.005

Ellsworth, P. V., & Sternberg, L. S. L. (2014). Biochemical effects of salinity on oxygen isotope fractionation during cellulose synthesis. *New Phytologist*, *202*(3), 784–789. https://doi.org/10.1111/nph.12696

Esper, J., Cook, E. R., Krusic, P. J., Peters, K., & Schweingruber, F. H. (2003). Tests of the RCS method for preserving low-frequency variability in long tree-ring chronologies. *Tree-Ring Research*, *59*, 81–98.

Esper, J., Frank, D. C., Battipaglia, G., Büntgen, U., Holert, C., Treydte, K., et al. (2010). Low-frequency noise in $\delta^{13}C$ and $\delta^{18}O$ tree ring data: A case study of *Pinus uncinata* in the Spanish pyrenees. *Global Biogeochemical Cycles*, *24*(4). https://doi.org/10.1029/2010GB003772

Esper, J., Krusic, P. J., Ljungqvist, F. C., Luterbacher, J., Carrer, M., Cook, E., et al. (2016). Ranking of tree-ring based temperature reconstructions of the past millennium. *Quaternary Science Reviews*, *145*, 134–151. https://doi.org/10.1016/j.quascirev.2016.05.009

Farquhar, G. D., von Caemmerer, S., & Berry, J. A. (1980). A biochemical model of photosynthetic CO_2 assimilation in leaves of C3 species. *Planta*, *149*(1), 78–90. https://doi.org/10.1007/BF00386231

Fowler, G. (1933). Shrinkage of the peat-covered Fenlands. *The Geographical Journal*, *81*(2), 149–150. https://doi.org/10.2307/1784565

Gessler, A., Ferrio, J. P., Hommel, R., Treydte, K., Werner, R. A., & Monson, R. K. (2014). Stable isotopes in tree rings: Towards a mechanistic understanding of isotope fractionation and mixing processes from the leaves to the wood. *Tree Physiology*, *34*(8), 796–818. https://doi.org/10.1093/treephys/tpu040

Glazebrook, J. (Ed.) (1997)., *Research and Archaeology: A Framework for the Eastern Counties 1. Resource assessment*. East Anglian Archaeology.

Godwin, H. (1940). Pollen analysis and forest history of England and Wales. *New Phytologist*, *39*(4), 370–400. https://doi.org/10.1111/j.1469-8137.1940.tb07149.x

Goslin, J., Fruergaard, M., Sander, L., Gałka, M., Menviel, L., Monkenbusch, J., et al. (2018). Holocene centennial to millennial shifts in North-Atlantic storminess and ocean dynamics. *Scientific Reports*, *8*(1), 12778. https://doi.org/10.1038/s41598-018-29949-8

Grudd, H., Briffa, K. R., Karlén, W., Bartholin, T. S., Jones, P. D., & Kromer, B. (2002). A 7400-year tree-ring chronology in northern Swedish Lapland: Natural climatic variability expressed on annual to millennial timescales. *The Holocene*, *12*(6), 657–665. https://doi.org/10.1191/0959683602hl578rp

Hansen, E. M., Reeser, P. W., & Sutton, W. (2012). Phytophthora beyond agriculture. *Annual Review of Phytopathology*, *50*(1), 359–378. https://doi.org/10.1146/annurev-phyto-081211-172946

Hantemirov, R. M., Corona, C., Guillet, S., Shiyatov, S. G., Stoffel, M., Osborn, T. J., et al. (2022). Current Siberian heating is unprecedented during the past seven millennia. *Nature Communications*, *13*(1), 4968. https://doi.org/10.1038/s41467-022-32629-x

Hantemirov, R. M., Shiyatov, S. G., Gorlanova, L. A., Kukarskih, V. V., Surkov, A. Y., Hamzin, I. R., et al. (2021). An 8768-year Yamal tree-ring chronology as a tool for paleoecological reconstructions. *Russian Journal of Ecology*, *52*(5), 419–427. https://doi.org/10.1134/S1067413621050088

Helama, S., Arppe, L., Timonen, M., Mielikäinen, K., & Oinonen, M. (2015). Age-related trends in subfossil tree-ring $\delta^{13}C$ data. *Chemical Geology*, *416*, 28–35. https://doi.org/10.1016/j.chemgeo.2015.10.019

Helama, S., Arppe, L., Timonen, M., Mielikäinen, K., & Oinonen, M. (2018). A 7.5 ka chronology of stable carbon isotopes from tree rings with implications for their use in palaeo-cloud reconstruction. *Global and Planetary Change*, *170*, 20–33. https://doi.org/10.1016/j.gloplacha.2018.08.002

Helama, S., Seppä, H., Bjune, A. E., & Birks, H. J. B. (2012). Fusing pollen-stratigraphic and dendroclimatic proxy data to reconstruct summer temperature variability during the past 7.5 ka in subarctic Fennoscandia. *Journal of Paleolimnology*, *48*(1), 275–286. https://doi.org/10.1007/s10933-012-9598-1

Hughes, M. K., & Graumlich, L. J. (1996). Multimillennial dendroclimatic studies from the western United States. In P. D. Jones, R. S. Bradley, & J. Jouzel (Ed.), *Climatic Variations and Forcing Mechanisms of the Last 2000 Years, NATO ASI Series* (pp. 109–124). Springer. https://doi.org/10.1007/978-3-642-61113-1_6

Iszkuło, G. (2010). Success and failure of endangered tree species: Low temperatures and low light availability affect survival and growth of European yew (*Taxus baccata* L.) seedlings. *Polish Journal of Ecology*, *58*.

Jackson, W. T. (1955). The role of adventitious roots in recovery of shoots following flooding of the original root systems. *American Journal of Botany*, *42*(9), 816–819. https://doi.org/10.2307/2438430

Kern, Z., Nagavciuc, V., Hatvani, I. G., Hegyi, I. N., Loader, N. J., & Popa, I. (2023). Evaluation of the non-climatic (age-related) trends of stable oxygen and carbon isotopes in Swiss stone pine (*Pinus cembra* L.) tree rings from the Eastern Carpathians, Romania. *Dendrochronologia*, *78*, 126061. https://doi.org/10.1016/j.dendro.2023.126061

Lara, A., Villalba, R., Urrutia-Jalabert, R., González-Reyes, A., Aravena, J. C., Luckman, B. H., et al. (2020). A 5680-year tree-ring temperature record for southern South America. *Quaternary Science Reviews*, *228*, 106087. https://doi.org/10.1016/j.quascirev.2019.106087

Leuschner, H. H., Sass-Klaassen, U., Jansma, E., Baillie, M. G. L., & Spurk, M. (2002). Subfossil European bog oaks: Population dynamics and long-term growth depressions as indicators of changes in the Holocene hydro-regime and climate. *The Holocene*, *12*(6), 695–706. https://doi.org/10.1191/0959683602hl584rp

Ljungqvist, F. C., Piermattei, A., Seim, A., Krusic, P. J., Büntgen, U., He, M., et al. (2020). Ranking of tree-ring based hydroclimate reconstructions of the past millennium. *Quaternary Science Reviews*, *230*, 106074. https://doi.org/10.1016/j.quascirev.2019.106074

Lovelock, C. E., Reef, R., & Ball, M. C. (2017). Isotopic signatures of stem water reveal differences in water sources accessed by mangrove tree species. *Hydrobiologia*, *803*(1), 133–145. https://doi.org/10.1007/s10750-017-3149-8

Macklin, M. G., Jones, A. F., & Lewin, J. (2010). River response to rapid Holocene environmental change: Evidence and explanation in British catchments. *Quaternary Science Reviews, Climate Variability of the British Isles and Adjoining Seas*, *29*(13–14), 1555–1576. https://doi.org/10.1016/j.quascirev.2009.06.010

Martínez-Sancho, E., Cernusak, L. A., Fonti, P., Gregori, A., Ullrich, B., Pannatier, E. G., et al. (2023). Unenriched xylem water contribution during cellulose synthesis influenced by atmospheric demand governs the intra-annual tree-ring $\delta^{18}O$ signature. *New Phytologist*, *240*(5), 1743–1757. https://doi.org/10.1111/nph.19278

McCarroll, D., & Loader, N. J. (2004). Stable isotopes in tree rings. *Quaternary Science Reviews, Isotopes in Quaternary Paleoenvironmental reconstruction*, *23*(7–8), 771–801. https://doi.org/10.1016/j.quascirev.2003.06.017

McCormac, F. G., Baillie, M. G. L., Pilcher, J. R., Brown, D. M., & Hoper, S. T. (1994). $\delta^{13}C$ measurements from the Irish oak chronology. *Radiocarbon*, *36*(1), 27–35. https://doi.org/10.1017/S0033822200014296

McKay, N. P., Kaufman, D. S., Arcusa, S. H., Kolus, H. R., Edge, D. C., Erb, M. P., et al. (2024). The 4.2 ka event is not remarkable in the context of Holocene climate variability. *Nature Communications*, *15*(1), 6555. https://doi.org/10.1038/s41467-024-50886-w

Medlycott, M. (Ed.) (2011)., *Research and Archaeology Revisited: A revised framework for the East of England*. East Anglian Archaeology.

Melvin, T. M. (2004). *Historical Growth Rates and Changing Climatic Sensitivity of Boreal Conifers*. University of East Anglia.

Miller, S. H., & Skertchly, S. B. J. (1878). The Fenland past and present.

Mott, K. A., Sibbernsen, E. D., & Shope, J. C. (2008). The role of the mesophyll in stomatal responses to light and CO_2. *Plant, Cell and Environment*, *31*(9), 1299–1306. https://doi.org/10.1111/j.1365-3040.2008.01845.x

Orr, P., Colvin, J., & King, D. (2007). Involving stakeholders in integrated river basin planning in England and Wales. *Water Resources Management*, *21*(1), 331–349. https://doi.org/10.1007/s11269-006-9056-9

Panyushkina, I. P., Leavitt, S. W., Thompson, T. A., Schneider, A. F., & Lange, T. (2008). Environment and paleoecology of a 12 ka mid-North American Younger Dryas forest chronicled in tree rings. *Quaternary Research*, *70*(3), 433–441. https://doi.org/10.1016/j.yqres.2008.08.006

Pilcher, J. R., Baillie, M. G. L., Brown, D. M., McCormac, F. G., Macsweeney, P. B., & McLawrence, A. S. (1995). Dendrochronology of subfossil pine in the North of Ireland. *Journal of Ecology*, *83*(4), 665–671. https://doi.org/10.2307/2261634

Reimer, P. J., Austin, W. E. N., Bard, E., Bayliss, A., Blackwell, P. G., Bronk Ramsey, C., et al. (2020). The IntCal20 northern Hemisphere radiocarbon age calibration curve (0–55 cal kBP). *Radiocarbon*, *62*(4), 725–757. https://doi.org/10.1017/RDC.2020.41

Roden, J. S., Lin, G., & Ehleringer, J. R. (2000). A mechanistic model for interpretation of hydrogen and oxygen isotope ratios in tree-ring cellulose. *Geochimica et Cosmochimica Acta*, *64*(1), 21–35. https://doi.org/10.1016/S0016-7037(99)00195-7

Roland, T. P., Caseldine, C. J., Charman, D. J., Turney, C. S. M., & Amesbury, M. J. (2014). Was there a "4.2 ka event" in Great Britain and Ireland? Evidence from the peatland record. *Quaternary Science Reviews*, *83*, 11–27. https://doi.org/10.1016/j.quascirev.2013.10.024

Salzer, M. W., Bunn, A. G., Graham, N. E., & Hughes, M. K. (2014). Five millennia of paleotemperature from tree-rings in the Great Basin, USA. *Climate Dynamics*, *42*(5–6), 1517–1526. https://doi.org/10.1007/s00382-013-1911-9

Saurer, M., Schweingruber, F., Vaganov, E. A., Shiyatov, S. G., & Siegwolf, R. (2002). Spatial and temporal oxygen isotope trends at the northern tree-line in Eurasia. *Geophysical Research Letters*, *29*(9), 7-1–7-4. https://doi.org/10.1029/2001GL013739

Scheidegger, Y., Saurer, M., Bahn, M., & Siegwolf, R. (2000). Linking stable oxygen and carbon isotopes with stomatal conductance and photosynthetic capacity: A conceptual model. *Oecologia*, *125*(3), 350–357. https://doi.org/10.1007/s004420000466

Shennan, I. (1986). Flandrian sea-level changes in the Fenland. I: The geographical setting and evidence of relative sea-level changes. *Journal of Quaternary Science*, *1*(2), 119–153. https://doi.org/10.1002/jqs.3390010204

Shennan, I., Bradley, S. L., & Edwards, R. (2018). Relative sea-Level changes and crustal movements in Britain and Ireland since the last glacial maximum. *Quaternary Science Reviews*, *188*, 143–159. https://doi.org/10.1016/j.quascirev.2018.03.031

Siegwolf, R. T. W., Lehmann, M. M., Goldsmith, G. R., Churakova, O. V., Mirande-Ney, C., Timoveeva, G., et al. (2023). Updating the dual C and O isotope—Gas-exchange model: A concept to understand plant responses to the environment and its implications for tree rings. *Plant, Cell and Environment*, *46*(9), 2606–2627. https://doi.org/10.1111/pce.14630

Sorrel, P., Debret, M., Billeaud, I., Jaccard, S. L., McManus, J. F., & Tessier, B. (2012). Persistent non-solar forcing of Holocene storm dynamics in coastal sedimentary archives. *Nature Geoscience*, *5*(12), 892–896. https://doi.org/10.1038/ngeo1619

Staubwasser, M., Sirocko, F., Grootes, P. M., & Segl, M. (2003). Climate change at the 4.2 ka BP termination of the Indus valley civilization and Holocene south Asian monsoon variability. *Geophysical Research Letters*, *30*(8). https://doi.org/10.1029/2002GL016822

Torbenson, M., Klippel, L., Hartl, C., Reinig, F., Treydte, K., Büntgen, U., et al. (2022). Investigation of age trends in tree-ring stable carbon and oxygen isotopes from northern Fennoscandia over the past millennium. *Quaternary International*, *631*, 105–114. https://doi.org/10.1016/j.quaint.2022.05.017

Torgeson, D. C., Young, R. A., & Milbrath, J. A. (1954). Phytophthora root rot diseases of Lawson cypress and other ornamentals.

Uścinowicz, S., Cieślikiewicz, W., Skrzypek, G., Zgrundo, A., Goslar, T., Jędrysek, M.-O., et al. (2022). Holocene relative water level and storminess variation recorded in the coastal peat bogs of the Vistula Lagoon, southern Baltic Sea. *Quaternary Science Reviews*, *296*, 107782. https://doi.org/10.1016/j.quascirev.2022.107782

Vornlocher, J. R., Lukens, W. E., Schubert, B. A., & Quan, C. (2021). Late Oligocene precipitation seasonality in east Asia based on $\delta^{13}C$ profiles in fossil wood. *Paleoceanography and Paleoclimatology*, *36*(4), e2021PA004229. https://doi.org/10.1029/2021PA004229

Walker, M., Head, M. J., Lowe, J., Berkelhammer, M., BjÖrck, S., Cheng, H., et al. (2019). Subdividing the Holocene series/epoch: Formalization of stages/ages and subseries/subepochs, and designation of GSSPs and auxiliary stratotypes. *Journal of Quaternary Science*, *34*(3), 173–186. https://doi.org/10.1002/jqs.3097

Waller, M. (1994). *The Fenland Project, Number 9: Flandrian environmental change in Fenland, East Anglian archaeology*. Cambridgeshire Archaeological Committee.

Wanner, H., Brönnimann, S., Casty, C., Gyalistras, D., Luterbacher, J., Schmutz, C., et al. (2001). North Atlantic Oscillation – Concepts and studies. *Surveys in Geophysics*, *22*, 321–381. https://doi.org/10.1023/A:1014217317898

Weiss, H., Courty, M.-A., Wetterstrom, W., Guichard, F., Senior, L., Meadow, R., & Curnow, A. (1993). The genesis and collapse of third millennium north mesopotamian civilization. *Science*, *261*(5124), 995–1004. https://doi.org/10.1126/science.261.5124.995

West, H., Quinn, N., & Horswell, M. (2019). Regional rainfall response to the North Atlantic Oscillation (NAO) across Great Britain. *Hydrology Research*, *50*(6), 1549–1563. https://doi.org/10.2166/nh.2019.015

West, H., Quinn, N., & Horswell, M. (2022). The influence of the North Atlantic Oscillation and East Atlantic pattern on drought in British catchments. *Frontiers of Environmental Science*, *10*. https://doi.org/10.3389/fenvs.2022.754597

Wieland, A., Römer, P., Torbenson, M., Greule, M., Urban, O., Čáslavský, J., et al. (2024). Tree-ring stable isotopes in cellulose and lignin methoxy groups reveal different age-related behaviour. *Quaternary International*, *693*, 38–48. https://doi.org/10.1016/j.quaint.2024.02.004

Yang, B., Qin, C., Bräuning, A., Osborn, T. J., Trouet, V., Ljungqvist, F. C., et al. (2021). Long-term decrease in Asian monsoon rainfall and abrupt climate change events over the past 6,700 years. *Proceedings of the National Academy of Sciences*, *118*(30), e2102007118. https://doi.org/10.1073/pnas.2102007118

Zander, P. D., Żarczyński, M., Tylmann, W., Vogel, H., & Grosjean, M. (2024). Subdecadal Holocene warm-season temperature variability in central Europe recorded by biochemical Varves. *Geophysical Research Letters*, *51*(22), e2024GL110871. https://doi.org/10.1029/2024GL110871